Interactive effects of seagrass and the microphytobenthos on sediment suspension within shallow coastal bays

Matthew A. Reidenbach* and Ross Timmerman

Department of Environmental Sciences, University of Virginia, Charlottesville, VA 22904, USA

*Corresponding author: telephone: 434-243-4937, email: reidenbach@virginia.edu

Abstract

The suspension and transport of sediments in coastal environments influences water column clarity, and also affects the growth of photosynthetic organisms. The presence of benthic vegetation, such as seagrass, can attenuate wave and tidal energy; thereby altering suspended sediment concentrations (SSC) and microphytobenthos (MPB) biomass that secrete biogenic compounds that can increase sediment cohesion. The dual role of seagrass and MPB in altering the seasonal critical bed shear stress, τ_c, necessary to suspend sediment was studied within a *Zostera marina* seagrass meadow and an adjacent unvegetated region within a shallow coastal bay in Virginia, USA. Hydrodynamics and MPB biomass were recorded seasonally to determine the critical bed shear stress and subsequent SSC response. Results show that seagrasses reduced mean currents and waves, thus lowering SSC within the meadow. In addition, seagrass created favorable conditions for MPB growth, with annual mean sediment carbohydrate concentrations, a proxy for MPB activity, to be double within the seagrass compared to the unvegetated site. Sediment carbohydrate concentrations within the seagrass bed were higher during winter than summer due to enhanced light penetration, which coincided with an increase in τ_c to 0.056 Pa compared to 0.024 Pa. τ_c was found to be 0.021 Pa at the unvegetated site, with bed shear exceeding this threshold >85% of the time. These findings suggest both MPB and seagrass play an important and interactive role in regulating seasonal sediment resuspension, and constant reworking of the bed sediments in high shear regions prevented the establishment of MPB.

Keywords: Eelgrass; Seagrass; Waves; Turbulence; Sediment; Microphytobenthos

Introduction

The transport of sediment in the marine environment is a universal process, altering the geomorphology of benthic and coastal systems and influencing ecosystem processes on varying spatial and temporal scales. For instance, suspended fine-grained particles and particulate matter can reduce water column light transmission, which limits the photosynthetic potential of primary producers, such as seagrasses and benthic microalgae (Lawson et al. 2007). However, suspension of sediments can also mix nutrients into the water column, making them available for primary producers (Cloern 2001). Sediment properties and the hydrodynamic forces imposed on these sediments are the primary factors controlling sediment suspension and transport. Energy from waves and tidal currents is transferred to the bed as a fluid shear stress (τ_b) and sediment suspension occurs when shear forces exceed gravitational, electromagnetic, and other cohesive forces acting on the bed material (Kimiaghalam et al. 2016). The shear threshold level that induces sediment suspension is known as the critical bed shear stress, τ_c (Teisson et al. 1993).

In general, smaller grained particles have a lower τ_c than larger grain sizes (Nielsen 1992), making them more likely to be mobilized. The critical bed shear stress has been readily predicted for sands (grain size >62.5 µm and <2 mm) and other larger grain sizes, when the grain size distribution is known (Wiberg and Smith 1987). Muds and other fine sediments (grain size <62.5 µm), however, have τ_c that are less predictable. These fine particles have electromagnetic properties, and on the seafloor may be intermixed with microscopic, photosynthetic algae and cyanobacteria, that form biofilms on the sediment surface that promote the binding of grains in a cohesive manner, which increases τ_c. (Friend et al. 2003a; Friend et al. 2003b; Miller et al. 1996). Although sands lack this characteristic and are classified as non-cohesive, certain sand to mud ratios also display cohesive properties (Houwing 1999). Other organisms, such as crabs, worms and other burrowers or tube builders, destabilize the surface through activities that increase the surface roughness or decrease τ_c (Eckman et al. 1981; Van Duren et al. 2006). This activity, compounded by their spatial and temporal variability (Andersen 2001; Lucas et al. 2003; Paterson et al. 2000; Underwood and Paterson 1993), renders τ_c inherently difficult to quantify. Ultimately, the magnitude of sediment that is suspended and transported is dependent on flow history, sediment and water properties, as well as biological activity at the seafloor (Mehta 1988; Mitchener and Torfs 1996; Paterson 1994; Salehi and Strom 2012).

Aggregations of benthic algae, bacteria and other photosynthetic microorganisms on sediment surfaces are classified as microphytobenthos (MPB). MPB support estuarine food webs and regulate nutrient fluxes across the seafloor (Douglass et al. 2011; McGlathery et al. 2012). In addition, microalgae are consumed by benthic invertebrates and fish and support significant secondary production in estuaries (Carpentier et al. 2014; Kuwae et al. 2012). The presence and activity of MPB result in the production of extracellular polymeric substances (EPS), a mucilaginous secretion broadly classified as a biopolymer. Several forms of EPS exist, but the general effect is twofold: it adheres to the sediment surface, attaching the MPB to the sediment, and it forms a coating around the MPB that provides a protective microenvironment (Decho 2000; Mariotti and Fagherazzi 2012; Weerman et al. 2010). Overall, EPS aids in the MPB colonization of the sediment surface and creates an inner microclimate capable of withstanding environmental extremes such as temperature, hydrodynamic forces, and other physical stresses found in coastal environments (e.g. Decho 2000). The accumulation of EPS on a sediment surface creates a network of interconnected grains (e.g. Patterson et al. 1991; Yallop et al. 1994), which stabilizes the surface as well as the MPB matrix (e.g. Black et al. 2002; Lucas et al. 2003), and subsequently increases τ_c. Many studies report peak benthic primary productivity during the spring and summer seasons, when insolation is high and temperatures approach the upper threshold of 30ºC (Carr et al. 2010; MacIntyre et al. 1996). However, MPB development in marine systems can also be adversely impacted by hydrodynamic conditions; where wave and tidal stresses can impart forces on the seafloor to cause reworking of the sediment surface, which limits MPB that contributes to cohesive bonding of sediments (Friend et al. 2003a; Lucas et al. 2003).

Numerous studies have also shown benthic vegetation, such as seagrass, reduce wave and current energy (Carr et al. 2010; Hansen and Reidenbach 2012; Peterson et al. 2004). The dissipation of energy leads to a reduction in bed shear stress (Bouma et al. 2009), promoting sediment deposition when settling forces exceed suspension forces (Adams et al. 2016; Gacia et al. 1999; Gruber and Kemp 2010). Bed shear stress in seagrass meadows is influenced by meadow characteristics such as vegetation density, blade length, and patchiness. Temperate seagrasses, such as *Zostera marina*, undergo seasonal growth cycles that alter the temporal and spatial extent of the meadow which, in turn, alters light penetration to the seafloor and their ability to dampen hydrodynamic energy (Hansen and Reidenbach 2013). Vegetation density and blade length are typically at a maximum during the spring growth and mid-summer biomass peak (Orth and McGlathery 2012). The minimum vegetation density occurs in winter when the blades slough off, leaving mostly belowground roots and rhizomes. When vegetation densities are high and blade lengths are long, the fluid energy is diverted over the meadow and away from the sediment (Hansen and Reidenbach 2017). When densities are low, hydrodynamic forces can penetrate through the meadow and enhance shear as the flow moves around individual blades (Lawson et al. 2012; Widdows et al. 2008). These seasonal variations in vegetation densities can have significant impacts on sediment dynamics and can also alter sediment bed properties and particle size distributions (van Katwijk et al. 2010; Ganthy et al. 2013). In wave environments, wave orbital motions cause the seagrass blades to oscillate forward and back on a timescale of seconds, allowing more wave energy to reach the bed (Hansen and Reidenbach 2013).

Since seagrass inhibits light availability to the sediment surface, it is expected that this shading will limit MPB biomass. Thus, sediment chlorophyll *a* and carbohydrate concentrations are expected to be lower compared to adjacent unvegetated surfaces where light is more abundant. However, hydrodynamic conditions are more quiescent and sediment stability is higher within seagrass beds, which is expected to create favorable conditions for MPB growth. Given these complex interactions, this study seeks to understand the role of MPB in seagrass dominated coastal bays and addresses the questions: (1) How does growth and senescence of the seagrass canopy impact wave development and bed shear stress within a shallow coastal bay? (2) How do variations in benthic chlorophyll *a* and carbohydrate (a proxy for MPB biomass) alter the critical bed shear stress? (3) What influence does seagrass have on benthic chlorophyll *a* and carbohydrate concentrations, and the τ_c necessary to suspend sediment?

Methods

Site Description

Measurements were conducted between January 2013 and June 2014 in South Bay, a micro-tidal estuary located along the Atlantic Ocean side of the Delmarva Peninsula, Virginia, USA (Figure 1). South Bay is part of the Virginia Coast Reserve (VCR) and is also a National Science Foundation Long Term Ecological Research (NSF–LTER) location. South Bay has an approximate area of 31.5 km^2, and an average water depth of 1.0 m at mean water level, but this water depth ranges between 0.25 m to 1.75 m due to tidal fluctuations. This site was chosen as the study location due to on-going seagrass restoration efforts (McGlathery et al. 2013; Orth et al. 2012; Orth et al. 2006). The dominant vegetation in South Bay is the seagrass (eelgrass) *Zostera marina*. Seagrasses, once a dominant feature in the coastal bays of the Delmarva Peninsula, disappeared in the 1930's due to a combination of a pandemic wasting disease and the 1933 Chesapeake-Potomac hurricane. Reseeding of South Bay with *Z. marina* occurred between 2001 – 2005. As of Summer 2010, the reseeded patches in South Bay had coalesced and grown to a meadow encompassing >6 km^2 (Orth et al. 2012). One location within the restored seagrass meadow (37.2635 N, 75.8224 W) and a separate unvegetated ('bare') control site (37.2677 N, 75.8280 W) were studied. The seagrass and bare site are separated by 0.8 km (Figure 1 inset). During summer-time conditions, maximum seagrass densities occur which typically range from 350-550 shoots m^{-2}, while in winter minimum seagrass densities occur due to senescence at approximately 100 shoots m^{-2} (Hansen and Reidenbach 2013). Seagrass densities were measured during winter 2013 and summer 2013 while experiments were conducted, and were found to be 100 ± 36 shoots m^{-2} and 411 ± 33 shoots m^{-2}, respectively (Reidenbach and Thomas 2018).

South Bay is bordered to the east by barrier islands and to the west by the Delmarva Peninsula. Narrow inlets between barrier islands restrict oceanic exchange. Turbidity is governed by local sediment resuspension by waves and currents, and the lack of significant freshwater sources does not introduce significant sediment loads. These characteristics allow for the assumption of a closed system in terms of sediment resuspension (Lawson et al. 2007). Waves are generated by wind stress over South Bay, where the average wind direction is from the SSE-SSW and N-NE directions (Fagherazzi and Wiberg 2009). The fetch lengths within South Bay vary depending upon wind direction and changes in water depth due to tidal fluctuations, but at mean water-depth, the N-S and E-W fetch lengths of South Bay are 7.5 km and 1-2 km, respectively. For north winds, fetch lengths at mean sea-level for the seagrass and bare site are 4.8 km and 4.5 km respectively, while for south winds fetch lengths for the seagrass and bare site are 2.7 km and 3.0 km, respectively. The largest waves in South Bay are typically formed during storm events with winds from the N-NE directions, with significant wave heights reaching 0.3 m (Reidenbach and Thomas 2018; Hansen and Reidenbach 2013). Winds from the east and west are unable to generate large waves due to the short fetch length and the presence of barrier islands and marsh that border South Bay. Wind data were obtained from a R.M. Young Wind Monitor anemometer located 5 km south of the site. Although there is some variability in the bathymetry, the mean water depth only varied by ±0.1 m across a 2 km long north to south transect within the seagrass meadow (Reidenbach and Thomas 2018).

Hydrodynamics and water quality parameters

A suite of hydrodynamic and water characteristics sensors were deployed at the seagrass and unvegetated sites for a minimum of 7 days during each season. Deployments took place in winter (January 21-29), spring (April 4-17), early summer (June 26-July 3), mid-summer (August 6-13), and fall (October 17-30) of 2013, and in the winter (February 20-March 4), spring (April 1-14) and early summer (May 27-June 4) of 2014. Current velocities (u, v, w) were obtained with a 6 MHz Nortek Vector acoustic Doppler velocimeter (ADV) measuring approximately 0.1 m above the bed at a sampling rate of 16 Hz. Velocity measurements were quantified at a single point within a 1 cm^3 sampling volume, and obtained in 10-minute bursts every 30 minutes, with 9600 samples per burst. To account for changes in flow patterns that might occur over Spring-Neap cycles, ADVs were simultaneously deployed at the seagrass and unvegetated sites for the duration of each seasonal deployment. Raw ADV data were filtered to remove samples with poor correlation (<85%) and low signal to noise ratio (SNR<25 dB). Data were also removed when the ADV velocity transducer was exposed to the air during low tide. The resulting velocity data were then converted from compass coordinates into u, v and w components, followed by a coordinate rotation where u is oriented in the direction of mean flow and the transverse (v) and vertical (z) components were minimized.

Water depth, tide and wave characteristics (wave period and significant wave height) were collected with Richard Brancker Research (RBR) model TWR-2050P wave gauges. These were positioned 0.1 m above the bed and adjacent to each ADV. The wave gauges recorded hydrostatic pressure for 1024 samples at a frequency of 4 Hz once every 10 min. Significant wave height for each wave record was obtained using the RBR wave analysis software (Ruskin) based on the variance of the 4-Hz depth-corrected water-surface elevation time series (Wiberg and Sherwood 2008). Suspended sediment concentrations were obtained with Campbell Scientific optical backscatter sensors (model OBS-3+). An OBS was coupled with each ADV and sampled at 16 Hz. The OBS sensors were positioned at the same depth as the ADV sampling volume (0.1 m above the bed). If necessary, a small patch of seagrass, roughly 0.2 m in diameter was removed from beneath the ADV and OBS sampling volumes to prevent interference with measurements. The sensors were previously calibrated to the sediment at each site (Hansen and Reidenbach 2012). Light and temperature loggers (Onset HOBO Pendant UA-002-64) were also deployed at the seagrass and bare sites. Two were positioned on each ADV instrument frame: one above the water surface and the other at the same depth as the ADV and OBS sampling volumes at 0.1 m above the seafloor. This allowed for the estimation of light levels both above and within the water column. Each logger recorded at 4-minute intervals. The loggers were calibrated with a photosynthetically active radiation (PAR) sensor using the procedure described by Long et al. (2012). A Yellow Springs Incorporated (YSI) model 6600 V2 water quality sonde was deployed 0.1 m above the bed at the seagrass site and measured temperature, salinity, pressure, pH, DO, turbidity, and water column chlorophyll *a*. Measurements were recorded at intervals of 4 minutes.

Microphytobenthos and sediment sampling

Replicate sediment samples were collected from the seagrass and bare sites with a modified 6 mL syringe (ID 12 x 50 mm length; core dimensions of ID 11.2 x 7.9 mm). The syringe was inserted into the sediment and the top 10 mm retained for analysis. Due to the rapid attenuation of light through sediment, sampling the upper 10 mm captures the bulk MPB population (e.g. Paterson et al. 2000). Sediment samples were stored in centrifuge tubes (15 mL BD Falcon) on ice and in the dark while in the field, and stored at -20 ºC after returning from the field. Colloidal carbohydrate samples were lyophilized within 24 hours of collection (Underwood et al. 1995).

Sediment samples were taken at the beginning and conclusion of each season from the seagrass and bare sites between January 2013 and June 2014. Samples were also collected over consecutive days during the summer deployments, with sampling separated by at least 1 hour to capture the benthic diel diatom migration and the different influences of tidal water depth and solar irradiance levels. In total, 124 sediment samples were collected and analyzed for chlorophyll, and 118 samples for carbohydrate. Chlorophyll samples were processed using the method described by Lorenzen (1967). In summary, 8 mL of a 45:45 methanol:acetone solution (10% dH_20) was added to each sample, sonicated for 1 minute, and allowed to extract overnight at -20 ºC. Following extraction, samples were centrifuged at 3660 rpm for 5 minutes and 3 mL of the supernatants were measured at 665 nm and 750 nm using a Shimadzu model UV-1800 spectrophotometer. The supernatants were then acidified with 0.25 mL 5% HCl and subsequently remeasured at both wavelengths to correct for phaeopigment content. Chlorophyll *a* and phaeopigments were calculated as (Lorenzen 1967):

$$chl\ a = 9.091 \times [26.73[(665_i - 750_i) - (665_a - 750_a)]v] \qquad (1)$$

$$phaeopigment = 9.091 \times [26.73[1.7(665_a - 750_a) - (665_i - 750_i)]v] \qquad (2)$$

where 665_i is the absorption at 665 nm prior to acidification, 750_i is the turbidity correction for 665_i, 665_a is absorption at 665 nm following acidification, 750_a is turbidity correction for 665_a, v is the volume (mL) of extract ($v = 8$ mL), and 9.091 is the conversion to mg m^{-2} of chlorophyll.

Colloidal carbohydrate samples were analyzed using the technique described by Underwood et al. (1995). This method incorporates the phenol-sulfuric acid assay (Dubois et al. 1956). In this standard technique, lyophilized sediment (0.5 ± 0.1 g) was extracted in saline (25‰) for 15 minutes at room temperature and centrifuged for 15 minutes at 3660 rpm. The supernatant (1 mL) was removed and placed in a glass test tube followed by 0.5 mL w/v 5% phenol and 2.5 mL H_2SO_4. The solution was incubated at room temperature for 30 minutes and the absorbance measured at 485 nm. The addition of phenol and sulfuric acid produces a yellow solution that is quantified by a glucose standard curve. Carbohydrate concentrations are therefore given in glucose equivalent (µg gl. eq. G^{-1} dry sed. wt).

Sediment characteristics were determined through seasonal sampling of 10 cm^3 cores (depth = 1.75 cm) at the vegetated center site and a nearby bare site. Three replicate cores were collected seasonally at each site. Each sample was sieved through a 2 mm screen and bleached to remove organic matter prior to analysis. Grain size was analyzed using a laser diffraction particle size analyzer (Beckman Coulter LS 13 320), which returned a grain size distribution curve. D_{84}

was determined from the curve as the diameter (D_x) at which 84% of the sample is finer than D_x. The annual mean D_{84} at the seagrass site was 155 ± 3 µm, and at the unvegetated site was 158 ± 3 µm. No statistical variation in sediment size was found across season at either the seagrass or unvegetated site.

Bed shear stress

Bed shear stress (τ_b) is defined as the frictional stress induced from fluid flow over the bed surface. In combined wave and current flows, the total shear stress is computed by (Wiberg and Smith 1983):

$$\tau_b = \sqrt{\tau_{wave}^2 + \tau_{current}^2} \tag{3}$$

where τ_{wave} is the bed shear due to waves and $\tau_{current}$ is the bed shear due to current. Indirect estimates of $\tau_{current}$ are only possible through velocity measurements made above the surface and extrapolating to the bed. Three common techniques are the log profile, turbulent kinetic energy (TKE), and the Reynolds stress methods (Reidenbach et al. 2006). The log profile technique (LP) assumes a constant stress layer, steady flow, logarithmic velocity profile, and a defined turbulent boundary layer exists (Kundu 1990). These characteristics typically do not apply in vegetated systems, therefore this technique was not applied. The Reynolds stress (RS) method uses the covariance of velocity fluctuations: $\tau_{current} = -\rho\left|\overline{u'w'}\right|$. This method assumes a constant Reynolds stress ($\overline{u'w'}$) within the inertial sublayer (Tennekes and Lumley 1972). Analysis of the flows measured within the seagrass and unvegetated sites showed that the RS technique is sensitive to noise fluctuations in measured $u'w'$, since fluctuations in the horizontal components of velocity from the ADV typically contain an order of magnitude more noise compared to vertical contributions (Kim et al. 2000).

A preferred method in vegetated systems is the TKE method, $\tau_{current} = C\rho E$, where $E = 0.5\left(\overline{u'^2} + \overline{v'^2} + \overline{w'^2}\right)$ is the turbulent kinetic energy, and $C=0.19$ is a proportionality constant (Kim et al. 2000; Stapleton and Huntley 1995; Verney et al. 2006). This approach assumes steady, current-dominated flows where turbulent fluctuations are attributed to currents only, and measurements are obtained within the constant stress layer. However, when waves are present, horizontal (u' and v') and vertical (w') contributions in wave orbital velocities lead to overestimates of TKE and shear. Under mixed wave-current conditions, an alternative is the modified TKE method (M-TKE), where only the vertical velocity fluctuations are considered:

$$\tau_{current} = 0.9\rho\overline{w'^2} \tag{4}$$

This approach requires a proportionality constant of 0.9, recommended by Kim et al. (2000), and has been shown to provide accurate measurements in wave-dominated systems (e.g. Salehi and Strom 2012), and is applied to our data.

Bed shear due to waves (τ_{wave}) was computed separately from the high frequency pressure signal from the wave gauges, described by Wiberg and Sherwood (2008):

$$\tau_{wave} = \frac{\rho f_w}{2} u_b^2 \quad f_w = 0.04\left[\frac{u_b T}{2\pi k_b}\right]^{-0.75} \tag{5}$$

where f_w is the friction factor, u_b is the bottom wave orbital velocity, T is the wave period, and k_b is the roughness length. Bottom orbital velocity u_b is estimated from linear wave theory by computing the horizontal wave orbital velocity at the seafloor:

$$u_b = \frac{\pi H}{T sinh(kh)} \tag{6}$$

where H is the significant wave height, k is the wave number, and h is the water depth. Roughness length k_b is estimated from the sediment grain size as $k_b = 3D_{84}$ (Lawson et al. 2007).

Significant wave heights less than 0.03 m were not included in the bed shear analysis, since they do not contribute to motions at the seafloor.

Determination of critical bed shear stress

Several relationships have been proposed to predict the critical bed shear stress of fine grain sediments (Mehta 1988; Mitchener and Torfs 1996; Verney et al. 2006) which have relied upon a combination of laboratory and in situ studies. However, collection, storage and transportation can alter biological and physical conditions of the sediment and impact results. Studies suggest more accurate results are obtained from in situ measurements (Black and Paterson 1997; Pope et al. 2006) due to the reduced surface disturbance of the bed. Within the seagrass bed, the critical bed shear was estimated utilizing simultaneous velocity and SSC measurement obtained during seasonal deployments measured at 0.1 m above the seafloor. τ_b (Eq. 3) was first estimated using the time series of velocities measured by the ADV and τ_c was determined as the bed shear conditions when sediment suspension was initiated. Sediment suspension was determined to have been initiated when SSC increased in magnitude ≥100% (i.e., a doubling) within a 30-min time period, that also coincided with a corresponding increase in τ_b. The mean bed shear stress measured during this time period was used as an estimate of τ_c. This technique of identifying the leading edge of suspension events and observing the corresponding bed shear stress is similar to that applied by Lawson et al. (2007) in an adjacent coastal bay.

Since previous measurements have shown that bed stresses at unvegetated sites in South Bay are often large enough to continually suspend sediment (Hansen and Reidenbach 2012), determination of τ_c using continuously recorded velocity and SSC is more problematic. The transition between flow conditions causing a shift from below to above τ_c typically only occurs during slack water, surrounding low and high tide. Therefore, to determine τ_c at the unvegetated site, an in situ flow-through flume was utilized. The flume (1.8 m L x 0.28 m W x 0.6 m H) consists of two vertical walls to channelize the flow, and was open on the bottom to allow the walls to penetrate into the bed (Figure 2). The walls were clear acrylic and secured to aluminum supports with low-profile bolts. The supports were outside of the flume channel. This design left the bed and water flow within the flume minimally disturbed. The flume was deployed at low tide and was oriented in the primary direction of tidal flow. Trials were performed during rising tide when velocities were increasing from below to above critical bed stress thresholds. Velocities were recorded with a 10 MHz Nortek Vectrino ADV at the downstream end of the channel. The ADV sampled approximately 0.1 m above the bed at 10 Hz. Turbidity was recorded at 1 Hz with Seapoint turbidity loggers placed within and outside ('ambient') the flume. Sediment samples were collected for chlorophyll *a* and carbohydrate analysis before and after each trial. Replicate trials were conducted after sediment suspension was observed. All trials were conducted when water depths were less than 0.6 m. The critical bed shear stress was identified when turbidity within the flume doubled due to a corresponding increase in shear stress, the same criteria used for τ_c determination at the seagrass site.

Hydrodynamic control experiments

The MPB growth response to an absence of shear was investigated utilizing clear cylindrical tubing (0.0825 m diameter x 0.61 m height) to prevent fluid velocities and shear stress from forming at the sediment-water interface. The tubing ('cylinder') was inserted 0.15 m (z) into the sediment, leaving 0.46 m (H) above the undisturbed sediment. The cylinder was secured to a PVC pole (0.019 m diameter) inserted 1.5 m into the bed to prevent movement and subsequent bed disturbance from cylinder movement. The cylinder deployment height to diameter (*H*:*D*) ratio was 5.5:1. This aspect ratio minimizes turbulence within the cylinder and reduces bed shear stresses (Storlazzi et al. 2011). Three replicates were deployed at the seagrass site for 11 days. The spacing between replicates was greater than 10*D* to prevent flow influence between cylinders (Storlazzi et al. 2011). The cylinders were continuously submerged for the duration of the experiment, allowing exchange of nutrients and dissolved oxygen with ambient water, and the clear material allowed sunlight to reach the benthic surface. Sediment samples were collected prior to deployment, and from within and outside of the cylinders after 11 days. Sediment was analyzed for chlorophyll *a* and carbohydrate concentrations. Cylinders were also deployed at the bare site, however the experiment was unsuccessful due to strong tidal currents, which destabilized the cylinders, causing scouring and removal of the cylinders from the bed.

Results

Physical characteristics in South Bay for each season are provided in Table 1. The mean seasonal wind speed ranged from 3.5±2.0 to 5.6±3.2 m s^{-1} and the dominant direction was from the north. There was no statistical significant difference in wind speed and direction during the study period (1-way ANOVA $p<0.01$). The average water temperature ranged from 4.4±2.0 °C in the winter to 26.7±1.8 °C during the summer. Salinity was nearly constant across all seasons, confirming no significant freshwater sources. Dissolved oxygen (DO) was also nearly constant throughout the study (1-way ANOVA $p<0.01$). The photosynthetically active radiation (PAR), measured above the water surface, did not vary across season, however the length of daily insolation did vary due to changing day length.

The average water depth seasonally ranged from 0.99 to 1.32 m at the seagrass site and from 0.88 to 1.09 m at the bare site. Variations seasonally within each site were primarily caused by changes in atmospheric pressure, neap-spring tidal fluctuations, wind setup and surge. Although of similar magnitude, seasonally averaged depths were greater at the seagrass site compared to the bare site (1-way ANOVA $p<0.05$). Tidal fluctuations were typically ±0.75 m around these average water depths. Currents in South Bay were tidally driven and influenced by the density of the seagrass meadow. Velocities at the seagrass site showed a seasonal trend (Figure 3A), where the average velocity in the winter (7.8 cm s^{-1}) was 2.7 times higher and statistically different (*t*-test $p<0.01$) than the summer (2.8 cm s^{-1}). Velocities generally did not exceed 20 cm s^{-1} during any season. Mean current velocities at the bare site were statistically similar across seasons, with a mean annual velocity of 12.8 cm s^{-1}.

The percent difference in mean velocity between the seagrass and unvegetated site is shown in Figure 3B. This measure can be used as a proxy to quantify the effect of the seagrass meadow on velocity reduction. Spring (April) and summer (May-June) were observed to have the largest velocity reductions while the lowest reductions were observed in winter (January and February). This trend corresponds to the seasonal growth cycle of seagrass, where peak densities occur in the spring and summer. Averaged over an annual cycle, the mean velocity at the seagrass site (Jan 2013 to May 2014) was 4.3 cm s^{-1}, while at the bare site the annual average was 12.8 cm s^{-1}. While average velocities were not statistically different between seasons at the unvegetated site, velocities did increase slightly in the spring (April) and summer (May-June).

Wave Characteristics

The seasonally averaged mean H_s ranged from 0.04 to 0.10 m for the seagrass site, while the unvegetated site had consistently higher mean H_s at 0.078 to 0.11 m (Figure 4A). Comparing seasonal differences between the two sites (Figure 4B), seasonally averaged H_s was statistically similar (*t*-test $p>0.05$) at the vegetated and bare sites during the winter (January 2013 and February 2014), with observed wave height reductions of <10%. However, during summer, wave heights were statistically different and approximately 40 to 50% lower at the seagrass site compared to the bare site (June and August 2013). At the seagrass site, mean H_s was 1.8 times greater in the winter compared to summer (0.10 m and 0.056 m, respectively), but there was no significant seasonal difference at the bare site (*t*-test $p>0.05$). Differences in wind speed and direction were not likely an important factor since there was no seasonal difference observed.

Critical bed shear stress

In total, 36 trials using the in situ flume were performed to determine the critical bed shear stress necessary to initiate sediment suspension at the unvegetated site. Of these, 17 showed clear signals of sediment suspension being initiated, coinciding with an increase in τ_b. Example results from two representative critical bed shear stress trials are shown in Figure 5. Increases in turbidity (black lines) were observed to follow increases in bed shear stress (blue lines and symbols). The turbidity response was delayed relative to the increase in shear in the trials by approximately 1 minute as the suspended sediment mixed vertically upwards and traversed the length of the flume to the turbidity sensor. Delays were consistent with flows of approximately 5 cm s^{-1} at a measured elevation of 0.1 m above the seafloor. Based on all the flume experiments with sediment suspension, a mean $\tau_c = 0.021$ Pa with a standard error (s.e.) of 0.005 Pa ($N = 17$) was found.

The critical bed shear stress was also examined in situ using the seasonal data from the seagrass bed (Table 2). The τ_c was identified using the same SSC criteria as the flume study, although there is considerable variability in the data due to the dynamics of the suspended sediment, that once suspended, it typically stays in suspension for hours to days. The τ_c values range from 0.024±0.015 (mean±s.e.) Pa in summer to 0.056±0.014 Pa in the winter, with a clear trend of higher τ_c values coinciding with time periods of lower seagrass biomass. On average, τ_c was found to be 2.3 times higher in the winter than summer.

Seasonal Bed Shear Stress

Boxplots of seasonal bed shear stress are presented in Figure 6. Red horizontal lines on the figure define the τ_c range of 0.02 to 0.05 Pa that were determined from the flume and seasonal analyses. Mean shear was greatest in January ($\tau_b = 0.05$ Pa) and lowest in April 2014 ($\tau_b = 0.019$ Pa) at the seagrass site, with an annual average of 0.03 Pa. In comparison, shear at the bare site was significantly greater throughout most of the study period (*t*-test $p<0.05$), with exception of January and October 2013 (*t*-test $p>0.05$) where shear was statistically similar. At the unvegetated site, the mean shear was highest in April 2013 ($\tau_b = 0.14$ Pa) and lowest in October ($\tau_b = 0.06$ Pa), with an annual average of 0.11 Pa. Shear values at the unvegetated site were statistically different between season (*t*-test $p<0.01$), while bed shear was statistically similar between seasons at the seagrass site (*t*-test $p>0.05$). Comparing the seagrass and unvegetated sites, the greatest difference in shear occurred in late spring and summer (statistically different, *t*-test $p<0.01$) due to flow and wave height reductions caused by the seagrass vegetation.

Figure 6C, 6D shows the percent of time during each season when shear stress exceeded the τ_c threshold values of either $\tau_c = 0.02$ Pa or 0.05 Pa at each site. Across all seasons, the shear stress at the seagrass site was 60% above the lower τ_c value of 0.02 Pa, and 20% above the upper range value of 0.05 Pa during the time periods of measurement. The shear stress at the bare site was above the lower τ_c value of 0.02 Pa during 88% of the time periods of measurement, and 71% above the upper range value of 0.05 Pa.

Suspended sediment concentrations

The mean seasonal suspended sediment concentrations (SSC) for both the seagrass and bare sites are shown in Figures 7A and 7B. The bare site had statistically higher SSC than the seagrass site when averaged annually (*t*-test $p<0.05$). While there was no statistical difference in mean SSC across seasons within the seagrass site (*t*-test $p>0.05$), at the bare site SSC was statistically higher in the summer than winter (*t*-test $p<0.05$). Water column chlorophyll was consistently below 10 μg L^{-1} throughout all seasons (Figure 7C) and therefore was only a minor contribution to overall turbidity levels that might impact subsurface PAR (Figure 7D). PAR levels measured near the seafloor varied primarily due to variations in water depth due to tidal fluctuations and turbidity caused by suspended sediment. The mean subsurface winter and summer PAR values measured at 0.1 m above the seafloor at the seagrass site were 1500 and 1300 μmol photons m^{-2} s^{-1}, respectively. At the bare site, the mean PAR measured at 0.1 m above the seafloor was 1300 and 960 μmol photons m^{-2} s^{-1} in the winter and summer, respectively. This suggests higher light levels were found at the seagrass than bare site at 0.1 m above the seafloor, primarily due to lower turbidity caused by suspended sediment. Values for PAR measured above the water surface are given in Table 1.

Benthic chlorophyll and carbohydrate concentrations

Seasonal sediment chlorophyll *a* concentrations for the seagrass and bare sites are shown in Figure 8A, 8B. In general, concentrations were slightly higher in the winter and early summer (June/May) and lower in the spring at the seagrass site, though differences were not statistically significant (1-way ANOVA, $p>0.05$). Lower solar insolation and water temperatures in the winter were anticipated to suppress growth, however concentrations were high compared to summer values. Chlorophyll concentrations were highest in January 2013 then declined through October 2013, which suggests the role of turbidity, and seagrass shading, in inhibiting light and MPB growth during the summer at the vegetated site.

The highest and lowest mean concentrations of sediment chlorophyll *a* at the bare site were in January (63.6 mg m^{-2}) and June (1.7 mg m^{-2}) 2013, respectively, but concentrations did not follow a seasonal trend. Comparing similar seasons, the concentration in January was at a maximum, while the following year in February they were nearly at a minimum (63.6 and 9.7 mg m^{-2}, respectively). This is likely due to increased storm activity in February 2014 that increased bed shear and prevented MPB expansion. Chlorophyll *a* concentrations in June 2013 were notably low, with the majority of sample replicates indicating an absence of chlorophyll (0 mg m^{-2}).

The sediment carbohydrate concentrations are presented in Figure 8C, 8D. The largest range was observed in April 2013 at both sites, most notably at the seagrass site. This may be because spring is a transition from winter to summer conditions. Concentrations were consistently higher at the seagrass site, with a mean concentration of 90.2 µg g^{-1}, while the bare site had an average carbohydrate concentration of 49.9 µg g^{-1}. Grouping seasons, mean concentrations were statistically different with higher values in the winter (104.59 µg g^{-1}) than summer (84.85 µg g^{-1}) (*t*-test $p<0.01$). At the bare site, concentrations were statistically similar except for a decrease in April 2014 (*t*-test $p<0.01$).

To determine the relationship between sediment chlorophyll and carbohydrate concentrations and the critical shear stress, sediment chlorophyll *a* and carbohydrate concentrations were grouped for both the bare and seagrass sites during each season, and compared to the mean τ_c across both sites (Figure 9). Although there is significant variability, τ_c was found to increase with increases in both chlorophyll *a* and carbohydrate concentrations. Separate linear fits were determined, which both indicate there is a statistically significant relationship ($p<0.01$) between increased MPB production and increases in τ_c.

Hydrodynamic control experiments

The MPB response to a low shear, high light environment was explored using the cylinder experiment (Table 3). Cylinders were deployed in August 2014 for an 11 day period when mean water temperatures were near the upper production threshold of 30º C. In the absence of shear and seagrass shading, at the end of the 11 day period sediment chlorophyll levels within the cylinder were 35% higher and statistically different (*t*-test $p<0.05$) compared to concentrations outside the cylinder. Sediment carbohydrate concentrations were 7 times higher within the cylinders and statistically different (*t*-test $p<0.01$) compared to outside of the cylinders. However, carbohydrate levels within the cylinders were only 23% higher than the concentrations measured during the start of the experiment (*t*-test $p>0.05$). The significant decrease in carbohydrate found between the start and end of the experiment within the seagrass meadow (outside of the cylinders), and high standard errors, reflect the ephemeral nature of extracellular secretions. However, it is possible that some of the carbohydrate measured is dead

MPB biomass (i.e. which may not contribute to a τ_c increase), since the cylinders stop the carbohydrates associated with dead MPB from being washed away. In comparison, sediment chlorophyll decreased only by 11% from beginning to end of the experiment (outside of the cylinders) and the standard errors were much smaller. Overall, the MPB response was positive in a low shear environment, increasing MPB biomass.

Discussion

Although there is large inherent variability in the dynamics of bed stress and suspended sediment due to changes in wave- and tidally-driven water velocities, there was a clear relationship between higher suspended sediment concentrations with larger bed shear stress, once a critical shear stress threshold was surpassed. This τ_c was found to vary both spatially and temporally within South Bay, and elevated values of τ_c were correlated with increased concentrations of MPB and aboveground seagrass biomass. Mean τ_c was found to be 0.021±0.005 (s.e., $n = 17$) Pa at the unvegetated site, and was correlated with relatively low benthic chlorophyll and carbohydrate concentrations compared to the seagrass site across all seasons. The shear stress at the bare site was found to be above the $\tau_c = 0.02$ Pa threshold for sediment suspension during 88% of the time periods of measurement. This bed stress above critical levels suggests a continual reworking of the bed sediments that likely prevented MPB from developing and thereby limiting the cohesiveness of the sediments through the development of EPS. At the seagrass site, τ_c seasonally ranged between 0.024 Pa in summer and 0.056 Pa in winter. Although there was temporal variability in MPB, sediment carbohydrate was statistically greater in the winter (104.59 $\mu g\ g^{-1}$) than summer (84.85 $\mu g\ g^{-1}$) as compared to 49.9 $\mu g\ g^{-1}$ measured at the bare site, which did not show statistically significant seasonal variations. This relationship between higher carbohydrate and greater τ_c is comparable to findings by Austen et al. (1999), who measured the erodibility of sediments along a mudflat transect.

Bed shear at the seagrass site was below the lower τ_c threshold of 0.2 Pa during 40% of the time periods of measurement, and below the upper $\tau_c = 0.05$ Pa during 80% of the time period of measurements. This stabilization of the bed due to the presence of seagrass suggested favorable physical conditions for growth of MPB. The hydrodynamic control experiments using clear plastic tubing confirmed that a low shear stress environment created large increases in MPB. Seagrass, such as *Z. marina*, reduce the hydrodynamic energy imposed at the seafloor, both due to a reduction in mean currents and waves (e.g. Bradley and Houser 2009; Hansen and Reidenbach 2012). However, seasonal seagrass growth cycles alter the hydrodynamic influence due to changes in above ground biomass (Hansen and Reidenbach 2013). Our results found significant wave height and current attenuation at the seagrass site compared to the adjacent unvegetated site. During winter, when seagrass biomass is near minimum, mean velocities were reduced by approximately 40-50%, while wave heights were only reduced by <10%. However, in late spring-summer during peak seagrass biomass, velocities were reduced by up to 150% and wave heights by 30-50% compared to the unvegetated site. Although wind direction across the coastal bay system provided a wide variety of fetch lengths to consider which may have impacted wave attenuation, these results are in general agreement with Reidenbach and Thomas (2018), who quantified similar wave height attenuation magnitudes across the seagrass canopy in South Bay over a much more limited range of north to south wind directions (wind direction of 22.5° to either side of due north). During spring-summer conditions, at the unvegetated site water velocities and SSC increased substantially, suggesting the drag and reduced flow imposed by the seagrass canopy created enhance flows over the bare site in South Bay, thereby increasing both bed shear stresses and SSC.

Potential other biological and physical factors controlling sediment dynamics

Although there are statistically significant correlations between increases in MPB and elevated critical shear stress, large seasonal variations in τ_c occurred within the seagrass bed for relatively modest changes in MPB. This suggests that there may be other co-occurring processes within the seagrass bed, both physical and biological, that could be impacting sediment stability (De Boer 2007). Alternative controls that may also enhance sediment stability within the seagrass are: (a) alterations to the nutrient and organic content of sediments, (b) changes in bioturbation due to seagrass density, (c) alterations in sediment stability due to rhizome structure, and (d) variations in water depth and circulation patterns that alter near bed flow conditions. Even though the range of critical bed shear stress measured in this study are of similar magnitude to previous studies within coastal bays in Virginia (Lawson et al. 2004; Lawson et al. 2012), they are substantially smaller than those measured within cohesive sediments in regions colonized by the seagrasses *Cymodocea nodosa* and *Zostera noltii* in Venice Lagoon, where critical stress thresholds ranged from 0.69 to 1.10 Pa (Amos et al. 2004). Although the cause for these differences are not certain, sediments in Venice Lagoon are comprised of substantially higher organic matter (25-50%) and at some sites, an approximately 1 mm thick surface biofilm layer.

Widdows et al. (2008) also found an increase in the critical bed shear stress within a seagrass canopy which was largely explained by an increase in MPB, but also due to a lower density of the grazer and bio-destabilizer *Hydrobia ulvae.* A field study by Fonseca (1989) measured sediment stabilization by a variety of seagrass species and found that *Halophila* *decipiens*, despite having substantially smaller leaf biomass than other seagrass species increased the threshold velocity for sediment motion. He found that beyond just aboveground leaf biomass, rhizomes that grow closer to the sediment-water interface can act as a physical driver for sediment stabilization. Therefore, the seagrass canopy itself could be impacting sediment properties, and near-bed biological processes other than MPB can additionally have a direct impact on τ_c and sediment erosion/deposition dynamics.

Variations in water depth and location within these shallow coastal bays likely also have a major impact on sediment erosion/deposition. The mean water depth at the seagrass site, that seasonally ranged from 0.99 to 1.32 m, was approximately 10% to 20% greater than that measured at the bare site (0.88 to 1.09 m). This variation may have an impact on near bed flow conditions. In general, tidally-driven flows in these shallow coastal bays are controlled through a balance between tidal excursion range and friction at the seafloor, with locations consisting of deeper water and closer to inlets typically associated with higher mean velocities and shorter residence times (Safak et al. 2015). Safak et al. (2015) modeled hydrodynamics within the VCR in the absence of benthic vegetation and predicted that the location of the seagrass site would have slightly higher mean velocities than the bare site. This suggests that the reduced mean velocities measured at the seagrass site are primarily due to the presence of vegetation.

The impact of differences in mean water depths at the two sites on wave statistics is less straightforward. Linear wave theory suggests waves will attenuate before reaching the seafloor for $f > \sqrt{g/(4\pi h)}$, where f is the wave frequency ($T = 1/f$) and h is the water depth (Wiberg & Sherwood 2008). Previous wave measurements in South Bay (Reidenbach and Thomas 2018) found that the wind waves formed over South Bay had relatively short wave periods that seasonally ranged from T= 1.6 to 2.4 s, but were not statistically different between the bare and seagrass sites. This range indicates that for similar wave conditions, a deeper water depth would experience smaller wave orbital velocities at the seafloor. Our results show that wave heights were statistically different and approximately 40 to 50% lower at the seagrass site compared to the bare site in summer, but not statistically different in winter. The equation describing the maximum wave orbital velocity at the seafloor is $u_b = \frac{\pi H}{T sinh(kh)}$ (Eq. 6) and indicates that, holding other wave characteristics constant, that lower wave heights and slightly deeper water depths at the seagrass site both act to reduce near-bed orbital velocities compared to the bare site. For the roughly 10 to 20% increase in mean water depths at the seagrass site compared to the bare site, and typical wave characteristics measured in South Bay, the increased water depth should also reduce wave orbital velocities at the seafloor by approximately 10 to 20%, while the decrease in wave height of 40 to 50% would reduce near bed orbital velocities by 40 to 50%. This suggests that wave height attenuation by the seagrass bed in summer has a greater impact on the reduction of wave orbital velocities than due to the deeper water depths. In winter, since wave heights are statistically similar, a deeper mean water depth at the seagrass site would tend to have a more prominent impact on reduced wave orbital velocities at the seafloor compared to the bare site.

Seasonal variations in seagrass, MPB, and shear stress

It was hypothesized that within the seagrass bed, higher average shear stresses in the winter may remove sediment chlorophyll and carbohydrate, however this was not observed. Higher chlorophyll/carbohydrate levels were observed in winter and early spring when seagrass density was minimal. While low water temperatures can suppress algal growth (Colijn and De Jonge 1984), the sparse seagrass meadow offset this effect by allowing more sunlight to reach the surface. The mean subsurface winter PAR for the seagrass site was 1500±800 μmol photons m^{-2} s^{-1}, while during the summer it was 1300±790 μmol photons m^{-2} s^{-1}. Although the bed shear stress measured at the seagrass site was not statistically different between seasons (Figure 6A), bed shear was found to be below critical stress levels for a greater proportion of time during winter than summer, even while factoring in the effects of elevated seagrass density in summer (Figure 6C). This combination of greater light penetration to the seafloor and enhanced bed stability likely created a positive feedback for MPB growth. Once developed, the higher chlorophyll and carbohydrate levels could then contribute to increased bed stability, which was reflected by a 2.3-fold increase in τ_c in winter compared to summer.

Due to the temporal and spatial variability in the chlorophyll and carbohydrate results, it is not possible to determine the relative importance of light availability or low bed shear in controlling MPB growth and activity in South Bay. While low light is a factor that can limit primary production, diatoms have been shown to be able to adapt to low light environments by increasing pigment production and light use efficiency (Cahoon 2014; García-Robledo et al. 2012). In addition, sediment grain size, hydrodynamic forces, and faunal grazing may all affect MPB at various spatial and temporal scales, leading to patch distributions and variable growth rates (Pratt et al. 2015; Weerman et al. 2010). Marine foundation species (such as dense communities of lugworms and mussels) have been found to increase MPB by attenuating hydrodynamic stresses and improve sediment stability (Donadi et al. 2013). However, macrofauna may also adversely impact MPB biomass and increase the erodibility of sediment through bioturbation (Orvain et al. 2014). We did not measure any impacts of grazing pressure or bioturbution on MPB biomass, and therefore, seasonal variations in these activities within the seagrass site may additionally impact both MPB and associated critical shear stresses.

A lower τ_c during summer could also be partially explained by increased fine sediment accumulation within the seagrass meadow due to hydrodynamic attenuation by the seagrass. There have been documented changes in sediment bed characteristics, namely the fining of sediments within the seagrass meadow as the meadow has developed over the past decade (McGlathery et al. 2012). Lower energy flows could enable the accumulation of fine sediments in the summer, making them more susceptible to suspension, and a lower τ_c, than in winter when grain sizes are larger. Previous measurements within the same seagrass bed found finer sediments within the seagrass canopy (130±17 μm) compared to an unvegetated site (157±7 μm) during summer time measurements in 2010 (Hansen and Reidenbach 2012). However, sediment samples collected during our experiments (in 2013 and 2014) showed no statistical difference in sediment size between the seagrass (155 ± 3 μm), and the unvegetated site (158 ± 3 μm). Likely, there is inherent spatial and temporal variability in sediment grain size within the seagrass bed that make conclusive statements regarding its overall effect on critical shear stress difficult.

Both seagrass and MPB have been shown independently to stabilize sediment surfaces through either hydrodynamic attenuation or increased sediment cohesion, respectively (Hansen and Reidenbach 2013; Friend et al. 2003a). Although the interactive effects of seagrass and MPB levels have not been previously reported, macroalgae and MPB have been found to interact in non-linear ways and compete for light and nutrients (Hardison et al. 2013). Recent measurements of MPB biomass in an adjacent coastal bay, also located within the Virginia Coast Reserve, found no consistent effect of macroalgae (*Gracilaria vermiculophylla*) biomass on MPB biomass (Besterman and Pace 2018). Even though this macroalgae can maintain large population densities throughout the year (Thomsen et al. 2006), due to its growth cycle and mobility, large seasonal and spatial variations in biomass occur (Besterman and Pace 2018). The ephemeral nature of *Gracilaria* may prevent it from having a significant impact on MPB, as compared to seagrass meadows which show a perennial aboveground biomass which enable for the reduction of currents and stabilization of the bed throughout the year.

Conclusion

While average shear stresses were statistically similar across seasons at the seagrass site, lower aboveground seagrass biomass led to higher light availability at the seafloor in winter vs. summer. Although other physical and biological drivers cannot be ruled out, this likely led to the increase in MPB biomass (chlorophyll and carbohydrate) and EPS, thereby increasing τ_c in winter vs. summer (0.056±0.014 and 0.024±0.015 Pa, *t*-test $p<0.01$). In addition, while high seagrass biomass conditions in summer are potentially detrimental to MPB biomass due to shading, it appears to still be beneficial to MPB growth by stabilizing the bed. The results of the hydrodynamic control cylinder experiments confirm that a high light and low shear stress environment is conducive to MPB productivity within this shallow coastal bay. These findings lead to a greater conceptual understanding of the integrated bio-physical system, where *Z. marina* and MPB both provide seasonal bed stabilization. Although seagrass does create shading of the seafloor, the dual effects of lowered suspended sediment concentrations and bed shear stresses within the canopy creates a positive feedback for MPB growth.

Acknowledgements

We thank A. Schwarzschild, C. Buck, and D. Boyd for field assistance. This research was funded by the National Science Foundation (NSF-DEB 1237733 and NSF-DEB 1832221) to the

Virginia Coast Reserve Long Term Ecological Research program and by a CAREER grant (NSF-OCE 1151314) to MAR.

References

Adams, M.P., R.K. Hovey, M.R. Hipsey, L.C. Bruce, M. Ghisalberti, R.J. Lowe, R.K. Gruber, L. Ruiz-Montoya, P.S. Maxwell, and D.P. Callaghan. 2016. Feedback between sediment and light for seagrass: Where is it important? *Limnology and Oceanography*.

Amos, C., A. Bergamasco, G. Umgiesser, S. Cappucci, D. Cloutier, L. DeNat, M. Flindt, M. Bonardi, and S. Cristante. 2004. The stability of tidal flats in Venice Lagoon—the results of in-situ measurements using two benthic, annular flumes. *Journal of Marine Systems* 51: 211-241.

Andersen, T. 2001. Seasonal variation in erodibility of two temperate, microtidal mudflats. *Estuarine, Coastal and Shelf Science* 53: 1-12.

Austen, I., T.J. Andersen, and K. Edelvang. 1999. The influence of benthic diatoms and invertebrates on the erodibility of an intertidal mudflat, the Danish Wadden Sea. *Estuarine, Coastal and Shelf Science* 49: 99-111.

Besterman, A.F., and M.L. Pace. 2018. Do Macroalgal Mats Impact Microphytobenthos on Mudflats? Evidence from a Meta-Analysis, Comparative Survey, and Large-Scale Manipulation. *Estuaries and Coasts*: 1-13.

Black, K., T. Tolhurst, D. Paterson, and S. Hagerthey. 2002. Working with natural cohesive sediments. *Journal of Hydraulic Engineering* 128: 2-8.

Black, K.S., and D.M. Paterson. 1997. Measurement of the erosion potential of cohesive marine sediments: a review of current in situ technology. *Journal of Marine Environmental Engineering* 4: 43-83.

Bouma, T.J., M. Friedrichs, P. Klaassen, B.K. van Wesenbeeck, F.G. Brun, S. Temmerman, M.M. van Katwijk, G. graf, and P.M.J. Herman. 2009. Effects of shoot stiffness, shoot size and current velocity on scouring sediment from around seedlings and propagules. *Marine Ecology Progress Series* 388: 293-297.

Bradley, K., and C. Houser. 2009. Relative velocity of seagrass blades: Implications for wave attenuation in low-energy environments. *Journal of Geophysical Research Earth Surfaces* 114: 1-13.

Cahoon, L.B. 2014. The role of benthic microalgae in neritic ecosystems. In *Oceanography and Marine Biology, An Annual Review, Volume 37*, 55-94: CRC Press.

Carpentier, A., S. Como, C. Dupuy, C. Lefrançois, and E. Feunteun. 2014. Feeding ecology of Liza spp. in a tidal flat: Evidence of the importance of primary production (biofilm) and associated meiofauna. *Journal of Sea Research* 92: 86-91.

Carr, J., P. D'Odorico, K. McGlathery, and P. Wiberg. 2010. Stability and bistability of seagrass ecosystems in shallow coastal lagoons: Role of feedbacks with sediment resuspension and light attenuation. *Journal of Geophysical Research: Biogeosciences (2005–2012)* 115.

Cloern, J.E. 2001. Our evolving conceptual model of the coastal eutrophication problem. *Marine Ecology Progress Series* 210: 223-253.

Colijn, F., and V.N. De Jonge. 1984. Primary production of microphytobenthos in the Ems-Dollard Estuary. *Marine Ecology Progress Series* 14: 185-196.

De Boer, W. 2007. Seagrass–sediment interactions, positive feedbacks and critical thresholds for occurrence: a review. *Hydrobiologia* 591: 5-24.

Decho, A.W. 2000. Microbial biofilms in intertidal systems: an overview. *Continental Shelf Research* 20: 1257-1273.

Donadi, S., J. Westra, E.J. Weerman, T. van der Heide, E.M. van der Zee, J. van de Koppel, H. Olff, T. Piersma, H.W. van der Veer, and B.K. Eriksson. 2013. Non-trophic interactions control benthic producers on intertidal flats. *Ecosystems* 16: 1325-1335.

Douglass, J.G., J.E. Duffy, and E.A. Canuel. 2011. Food web structure in a Chesapeake Bay eelgrass bed as determined through gut contents and 13C and 15N isotope analysis. *Estuaries and Coasts* 34: 701-711.

Dubois, M., K.A. Gilles, J.K. Hamilton, P.t. Rebers, and F. Smith. 1956. Colorimetric method for determination of sugars and related substances. *Analytical Chemistry* 28: 350-356.

Eckman, J.E., A.R. Nowell, and P.A. Jumars. 1981. Sediment destabilization by animal tubes. *Journal of Marine Research* 39: 361-373.

Fagherazzi, S., and P. Wiberg. 2009. Importance of wind conditions, fetch, and water levels on wave-generated shear stresses in shallow intertidal basins. *Journal of Geophysical Research* 114.

Fonseca, M. 1989. Sediment stabilization by *Halophila decipiens* in comparison to other seagrasses. *Estuarine, Coastal and Shelf Science* 29: 501-507.

Friend, P., P. Ciavola, S. Cappucci, and R. Santos. 2003a. Bio-dependent bed parameters as a proxy tool for sediment stability in mixed habitat intertidal areas. *Continental Shelf Research* 23: 1899-1917.

Friend, P., M. Collins, and P. Holligan. 2003b. Day–night variation of intertidal flat sediment properties in relation to sediment stability. *Estuarine, Coastal and Shelf Science* 58: 663-675.

Gacia, E., T. Granata, and C. Duarte. 1999. An approach to measurement of particle flux and sediment retention within seagrass (Posidonia oceanica) meadows. *Aquatic Botany* 65: 255-268.

Ganthy, F., A. Sottolichio, and R. Verney. 2013. Seasonal modification of tidal flat sediment dynamics by seagrass meadows of *Zostera noltii* (Bassin d'Arcachon, France). *Journal of Marine Systems* 109: S233-S240.

García-Robledo, E., A. Corzo, S. Papaspyrou, and E.P. Morris. 2012. Photosynthetic activity and community shifts of microphytobenthos covered by green macroalgae. *Environmental Microbiology Reports* 4: 316-325.

Gruber, R.K., and W.M. Kemp. 2010. Feedback effects in a coastal canopy-forming submersed plant bed. *Limnology and Oceanography* 55(6): 2285-2298.

Hansen, J.C., and M.A. Reidenbach. 2013. Seasonal growth and senescence of a Zostera marina seagrass meadow alters wave-dominated flow and sediment suspension within a coastal bay. *Estuaries and Coasts* 36: 1099-1114.

Hansen, J.C., and M.A. Reidenbach. 2017. Turbulent mixing and fluid transport within Florida Bay seagrass meadows. *Advances in Water Resources* 108: 205-215.

Hansen, J.C.R., and M.A. Reidenbach. 2012. Wave and tidally driven flows in eelgrass beds and their effect on sediment suspension. *Marine Ecology Progress Series* 448: 271-287.

Hardison, A., E. Canuel, I. Anderson, C. Tobias, B. Veuger, and M. Waters. 2013. Microphytobenthos and benthic macroalgae determine sediment organic matter composition in shallow photic sediments. *Biogeosciences* 10: 5571.

Houwing, E.-J. 1999. Determination of the critical erosion threshold of cohesive sediments on intertidal mudflats along the Dutch Wadden Sea coast. *Estuarine, Coastal and Shelf Science* 49: 545-555.

Kim, S.C., C.T. Friedrichs, J.P.Y. Maa, and L.D. Wright. 2000. Estimating bottom stress in tidal boundary layer from acoustic Doppler velocimeter data. *Journal of Hydraulic Engineering* 126: 399-406.

Kimiaghalam, N., S.P. Clark, and H. Ahmari. 2016. An experimental study on the effects of physical, mechanical, and electrochemical properties of natural cohesive soils on critical shear stress and erosion rate. *International Journal of Sediment Research* 31: 1-15.

Kundu, P. 1990. *Fluid Mechanics*. New York, NY: Academic Press.

Kuwae, T., E. Miyoshi, S. Hosokawa, K. Ichimi, J. Hosoya, T. Amano, T. Moriya, M. Kondoh, R.C. Ydenberg, and R.W. Elner. 2012. Variable and complex food web structures revealed by exploring missing trophic links between birds and biofilm. *Ecology Letters* 15: 347-356.

Lawson, S., K. McGlathery, and P. Wiberg. 2012. Enhancement of sediment suspension and nutrient flux by benthic macrophytes at low biomass. *Marine Ecology Progress Series* 448: 259-270.

Lawson, S.E., P.L. Wiberg, K.J. McGlatherty, and D.C. Fugate. 2007. Wind-driven sediment suspension controls light availability in a shallow coastal lagoon. *Estuaries and Coasts* 30: 102-112.

Long, M.H., J.E. Rheuban, P. Berg, and J.C. Zieman. 2012. A comparison and correction of light intensity loggers to photosynthetically active radiation sensors. *Limnology and Oceanography: Methods* 10: 416-424.

Lorenzen, C.J. 1967. Determination of chlorophyll and pheo-pigments: spectrophotometric equations. *Limnology and Oceanography* 12: 343-346.

Lucas, C.H., J. Widdows, and L. Wall. 2003. Relating spatial and temporal variability in sediment chlorophylla and carbohydrate distribution with erodibility of a tidal flat. *Estuaries* 26: 885-893.

MacIntyre, H.L., R.J. Geider, and D.C. Miller. 1996. Microphytobenthos: the ecological role of the “secret garden” of unvegetated, shallow-water marine habitats. I. Distribution, abundance and primary production. *Estuaries* 19: 186-201.

Mariotti, G., and S. Fagherazzi. 2012. Modeling the effect of tides and waves on benthic biofilms. *Journal of Geophysical Research: Biogeosciences* 117.

McGlathery, K., L. Reynolds, L. Cole, R. Orth, S. Marion, and A. Schwarzschild. 2012. Recovery trajectories during state change from bare sediment to eelgrass dominance. *Marine Ecology Progress Series* 448: 209-221.

McGlathery, K.J., M.A. Reidenbach, P. D'Odorico, S. Fagherazzi, M.L. Pace, and J.H. Porter. 2013. Nonlinear dynamics and alternative stable states in shallow coastal systems. *Oceanography* 26: 220-231.

Mehta, A. 1988. Laboratory studies on cohesive sediment deposition and erosion. In *Physical Processes in Estuaries*, 427-445: Springer.

Miller, D.C., R.J. Geider, and H.L. MacIntyre. 1996. Microphytobenthos: the ecological role of the “secret garden” of unvegetated, shallow-water marine habitats. II. Role in sediment stability and shallow-water food webs. *Estuaries* 19: 202-212.

Mitchener, H., and H. Torfs. 1996. Erosion of mud/sand mixtures. *Coastal engineering* 29: 1-25.

Nielsen, P. 1992. *Coastal Bottom Boundary Layers and Sediment Transport*: World Scientific.

Orth, R.J., T.J. Carruthers, W.C. Dennison, C.M. Duarte, J.W. Fourqurean, K.L. Heck, A.R. Hughes, G.A. Kendrick, W.J. Kenworthy, and S. Olyarnik. 2006. A global crisis for seagrass ecosystems. *Bioscience* 56: 987-996.

Orth, R., K. Moore, S. Marion, D. Wilcox, and D. Parrish. 2012. Seed addition facilitates eelgrass recovery in a coastal bay system. *Marine Ecology Progress Series* 448: 177-195.

Orth, R.J., M.L. Luckenbach, S.R. Marion, K.A. Moore, and D.J. Wilcox. 2006. Seagrass recovery in the Delmarva coastal bays, USA. *Aquatic Botany* 84: 26-36.

Orth, R.J., and K.J. McGlathery. 2012. INTRODUCTION: Eelgrass recovery in the coastal bays of the Virginia Coast Reserve, USA. *Marine Ecology Progress Series* 448: 173-176.

Orvain, F., K. Guizien, S. Lefebvre, M. Bréret, and C. Dupuy. 2014. Relevance of macrozoobenthic grazers to understand the dynamic behaviour of sediment erodibility and microphytobenthos resuspension in sunny summer conditions. *Journal of Sea Research* 92: 46-55.

Paterson, D. 1994. Biological mediation of sediment erodibility: ecology and physical dynamics. *Cohesive Sediments*.

Paterson, D., T. Tolhurst, J. Kelly, C. Honeywill, E. De Deckere, V. Huet, S. Shayler, K. Black, J. De Brouwer, and I. Davidson. 2000. Variations in sediment properties, Skeffling mudflat, Humber Estuary, UK. *Continental Shelf Research* 20: 1373-1396.

Patterson, M.R., K.P. Sebens, and R.R. Olson. 1991. In situ measurements of flow effects on primary production and dark respiration in reef corals. *Limnology and Oceanography* 36: 936-948.

Peterson, C.H., R.A. Luettich, F. Micheli, and G.A. Skilleter. 2004. Attenuation of water flow inside seagrass canopies of differing structure. *Marine Ecology Progress Series* 268: 81-92.

Pope, N.D., J. Widdows, and M.D. Brinsley. 2006. Estimation of bed shear stress using the turbulent kinetic energy approach: a comparison of annular flume and field data. *Continental Shelf Research* 26: 959-970.

Pratt, D.R., C.A. Pilditch, A.M. Lohrer, S.F. Thrush, and C. Kraan. 2015. Spatial distributions of grazing activity and microphytobenthos reveal scale-dependent relationships across a sedimentary gradient. *Estuaries and Coasts* 38: 722-734.

Reidenbach, M.A., S.G. Monismith, J.R. Koseff, G. Yahel, and A. Genin. 2006. Boundary layer turbulence and flow structure over a fringing coral reef. *Limnology and Oceanography* 51: 1956-1968.

Reidenbach, M.A., and E.L. Thomas. 2018. Influence of the seagrass, *Zostera marina*, on wave attenuation and bed shear stress within a shallow coastal bay. *Frontiers in Marine Science* 5: 397.

Safak, I., P. Wiberg, D. Richardson, and M. Kurum. 2015. Controls on residence time and exchange in a system of shallow coastal bays. *Continental Shelf Research* 97: 7-20.

Salehi, M., and K. Strom. 2012. Measurement of critical shear stress for mud mixtures in the San Jacinto estuary under different wave and current combinations. *Continental Shelf Research* 47: 78-92.

Stapleton, K.R., and D.A. Huntley. 1995. Seabed stress determinations using the inertial dissipation method and the turbulent kinetic energy method. *Earth Surface Processes and Landforms* 20: 807-815.

Storlazzi, C., M. Field, and M. Bothner. 2011. The use (and misuse) of sediment traps in coral reef environments: theory, observations, and suggested protocols. *Coral Reefs* 30: 23-38.

Teisson, C., M. Ockenden, P. Le Hir, C. Kranenburg, and L. Hamm. 1993. Cohesive sediment transport processes. *Coastal Engineering* 21: 129-162.

Tennekes, H., and J. Lumley. 1972. *A First Course in Turbulence*. Cambrindge, Massachusetts: The MIT Press.

Thomsen, M.S., K.J. McGlathery, and A.C. Tyler. 2006. Macroalgal distribution patterns in a shallow, soft-bottom lagoon, with emphasis on the nonnativeGracilaria vermiculophylla andCodium fragile. *Estuaries and Coasts* 29: 465-473.

Underwood, G.J., and D.M. Paterson. 1993. Seasonal changes in diatom biomass, sediment stability and biogenic stabilization in the Severn Estuary. *Journal of the Marine Biological Association of the United Kingdom* 73: 871-887.

Underwood, G.J.C., D.M. Paterson, and R.J. Parkes. 1995. The measurement of microbial carbohydrate exoploymers from intertidal sediments. *Limnology and Oceanography* 40: 1243-1253.

Van Duren, L.A., P.M. Herman, A.J. Sandee, and C.H. Heip. 2006. Effects of mussel filtering activity on boundary layer structure. *Journal of Sea Research* 55: 3-14.

Van Katwijk, M., A. Bos, D. Hermus, and W. Suykerbuyk. 2010. Sediment modification by seagrass beds: Muddification and sandification induced by plant cover and environmental conditions. *Estuarine, Coastal and Shelf Science* 89: 175-181.

Verney, R., J.-C. Brun-Cottan, R. Lafite, J. Deloffre, and J. Taylor. 2006. Tidally-induced shear stress variability above intertidal mudflats in the macrotidal Seine Estuary. *Estuaries and Coasts* 29: 653-664.

Weerman, E.J., J. Van de Koppel, M.B. Eppinga, F. Montserrat, Q.-X. Liu, and P.M. Herman. 2010. Spatial self-organization on intertidal mudflats through biophysical stress divergence. *The American Naturalist* 176: E15-E32.

Wiberg, P., and J.D. Smith. 1983. A comparison of field data and theoretical models for wave current interactions at the bed on the continental shelf. *Continental Shelf Research* 2: 147-162.

Wiberg, P.L., and C.R. Sherwood. 2008. Calculating wave-generated bottom orbital velocities from surface-wave parameters. *Computers and Geosciences* 34: 1243-1262.

Wiberg, P.L., and J.D. Smith. 1987. Calculations of the critical shear stress for motion of uniform and heterogeneous sediments. *Water Resources Research* 23: 1471-1480.

Widdows, J., N.D. Pope, M.D. Brinsley, H. Asmus, and R.M. Asmus. 2008. Effects of seagrass beds (*Zostera noltii* and *Z. marina*) on near-bed hydrodynamics and sediment resuspension. *Marine Ecology Progress Series* 358: 125-136.

Yallop, M.L., B. de Winder, D.M. Paterson, and L.J. Stal. 1994. Comparative structure, primary production and biogenic stabilization of cohesive and non-cohesive marine sediments inhabited by microphytobenthos. *Estuarine, Coastal and Shelf Science* 39: 565-582.

Tables

Table 1. Seasonal mean wind speed (±s.d.), wind direction, photosynthetically active radiation (PAR) measured above the water surface, water temperature (±s.d.), salinity (±s.d.) and dissolved oxygen (±s.d.).

Date	Wind Speed ($m\ s^{-1}$)	Wind Dir. (deg.)	PAR (μmol photons $m^{-2}\ s^{-1}$)	Temp. (°C)	Salinity (PSU)	DO (% sat)
Jan 2013	4.4±2.5	27	N/A	4.3±2.0	30.3±0.3	100.8±6.4
Apr 2013	4.9±2.0	336	1700	15.0±3.4	N/A	N/A
Jun 2013	4.8±1.6	313	1460	24.9±1.7	30.6±2.9	103.0±26.4
Aug 2013	3.6±1.8	312	2240	26.7±1.8	32.2±0.6	104.7±24.8
Oct 2013	3.5±2.0	19	2220	17.0±2.8	29.3±0.8	102.0±9.3
Feb 2014	5.6±3.2	46	2150	5.5±2.5	30.6±0.2	101.5±7.0
Apr 2014	4.3±1.7	333	N/A	13.4±2.4	31.5±0.2	108.9±15.0
May 2014	4.6±2.3	303	2280	22.1±2.3	30.7±0.3	118.5±28.8

Table 2. Summary of seasonal τ_c values measured at the seagrass site (mean ± s.e.).

	Jan 2013	Jun 2013	Oct 2013	Feb 2014	Apr 2014	May 2014
τ_c (Pa)	0.056±0.014	0.024±0.015	0.031±0.025	0.052±0.045	0.033±0.027	0.033±0.026

Table 3: Chlorophyll and carbohydrate concentrations (mean ± s.e.) at the seagrass site both outside of and within clear cylinders used as a hydrodynamic control, measured during deployment (initial concentrations) and recovery (final concentrations) of the cylinders across an 11 day period (*n* = 3).

	initial concentration (outside cylinder)	final concentration (outside cylinder)	final concentration (within cylinder)
Chlorophyll ($mg\ m^{-2}$)	43.0±1.3	38.3±8.9	51.8±7.3
Carbohydrate ($\mu g\ g^{-1}$)	236.7±114.0	36.2±7.7	291.0±50.0

Figure legends

Figure 1. Map of the study location and South Bay site coordinates. The white outline in the right subfigure indicates the seagrass meadow extent as of 2010 (Orth et al. 2012).

Figure 2. Diagram of in situ flume used to determine the critical bed shear stress.

Figure 3. (A) Mean seasonal velocities for the seagrass (green) and bare (black) sites with ±1 standard deviation. The standard deviation is shown to signify the range in velocities during each season due to tidal fluctuations and other forcing mechanisms. (B) Percent reduction in mean velocity at the seagrass site relative to the unvegetated site.

Figure 4. (A) The mean seasonal H_s at the seagrass (green) and adjacent bare (black) sites with ±1 standard deviation. The standard deviation is shown to signify the range in H_s during each season due to variations in wind magnitude and other forcing mechanisms. (B) Percent differences in mean H_s between the seagrass and unvegetated site.

Figure 5. Time-series of shear stress (blue) and turbidity (black) from two flume trials at the unvegetated site to determine τ_c. The red horizontal lines denote a shear stress of 0.04 Pa estimated by Lawson et al. (2007).

Figure 6. Boxplot of seasonal bed shear stress for the (A) seagrass and (B) unvegetated sites. The red horizontal lines mark the τ_c range of 0.02 to 0.05 Pa. Central lines within each box

represents the median, the bottom and top box limits are the 25th and 75th percentiles, respectively. Whiskers are the minima and maxima. Shear stress could not be calculated at the seagrass site in August due to poor ADV signal quality. (C) Percent of time above the τ_c range of 0.02 Pa to 0.05 Pa for the seagrass and (D) bare sites for each seasonal deployment.

Figure 7. Boxplot of seasonal suspended sediment concentrations (SSC) for the (A) seagrass and (B) bare sites, (C) water column chlorophyll levels measured at the seagrass site, and (D) average water column PAR levels at the seagrass (green line) and bare sites (black line). Central lines within each box represents the median, the bottom and top box limits are the 25th and 75th percentiles, respectively. Whiskers are the minima and maxima.

Figure 8. Boxplot of seasonal benthic chlorophyll *a* from the (A) seagrass and (B) bare sites. Boxplot of seasonal benthic colloidal carbohydrate from the (C) seagrass and (D) bare sites. Central lines within each box represents the median, the bottom and top box limits are the 25th and 75th percentiles, respectively. Whiskers are the minima and maxima not considered outliers, and the red crosses are outliers. No carbohydrate data was collected during January 2013 at either the seagrass or bare site.

Figure 9. Mean seasonal relationship between τ_c, chlorophyll *a* (green) and carbohydrate (dark green) with standard error, combined for seagrass and bare sites. Data points represent the mean sediment chlorophyll *a* or carbohydrate concentrations within each season for both the bare and seagrass sites combined, and compared to the mean τ_c. Both the chlorophyll *a* and carbohydrate

best-fit lines indicate a statistically significant relationship ($p<0.01$) between increases in MPB with increases in τ_c.

Figure 1

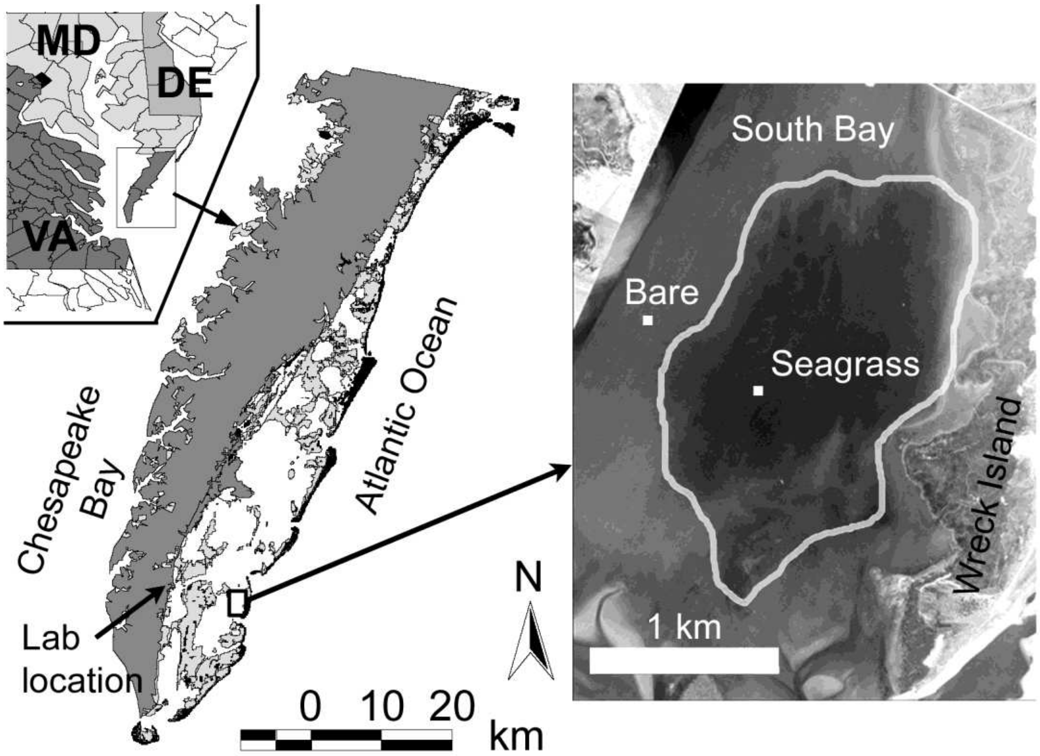

MD
DE
VA
Chesapeake Bay
Atlantic Ocean
Lab location
0 10 20
km
N
South Bay
Bare
Seagrass
Wreck Island
1 km

Figure 2

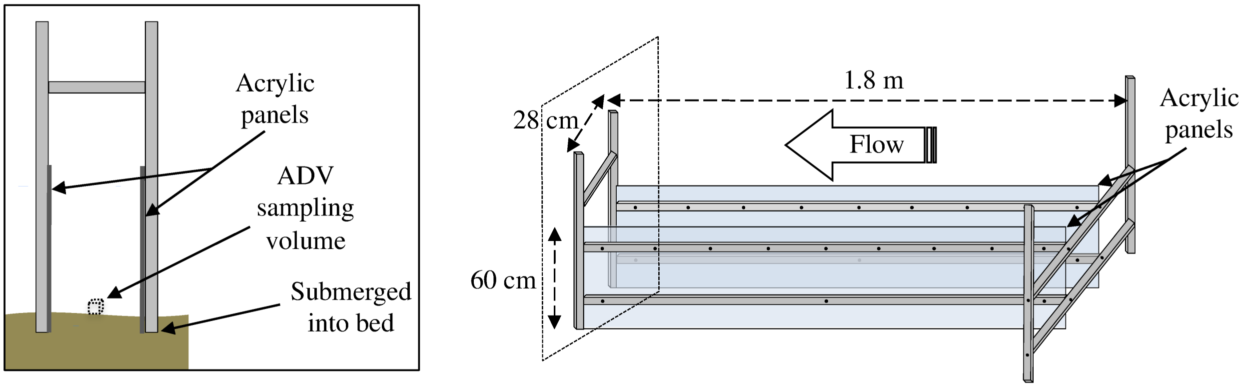
Acrylic panels
ADV sampling volume
Submerged into bed
1.8 m
28 cm
Flow
60 cm
Acrylic panels

Figure 3

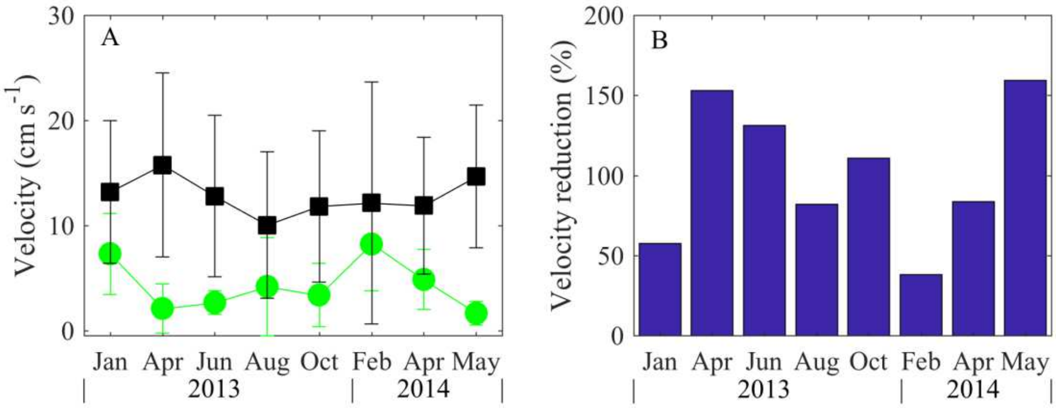
A
Velocity (cm s^{-1})
0
10
20
30
B
Velocity reduction (%)
0
50
100
150
200
Jan
Apr
Jun
Aug
Oct
Feb
Apr
May
2013
2014

Figure 4

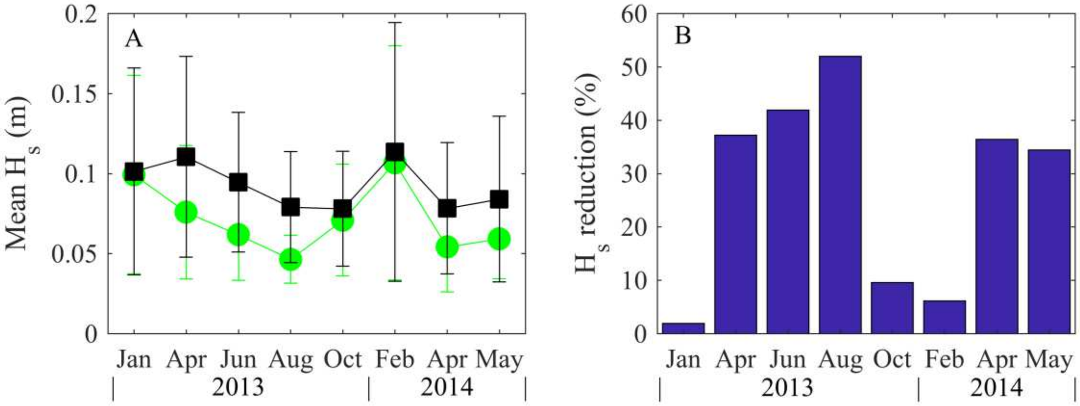
A
Mean H_s (m)
0.2
0.15
0.1
0.05
0
Jan
Apr
Jun
Aug
Oct
Feb
Apr
May
2013
2014
B
H_s reduction (%)
60
50
40
30
20
10
0
Jan
Apr
Jun
Aug
Oct
Feb
Apr
May
2013
2014

Figure 5

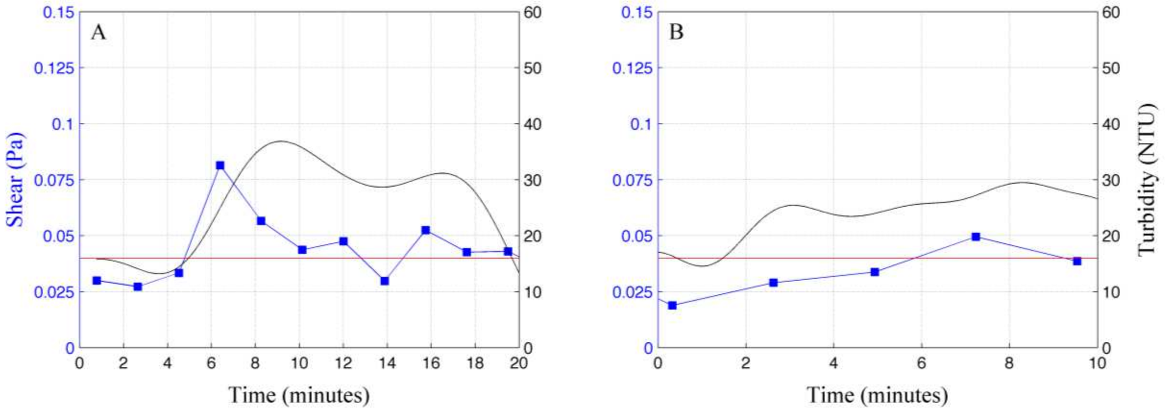
A
B
Shear (Pa)
Turbidity (NTU)
Time (minutes)
Time (minutes)
0.15
0.125
0.1
0.075
0.05
0.025
0
60
50
40
30
20
10
0
0
2
4
6
8
10
12
14
16
18
20
0
2
4
6
8
10

Figure 6

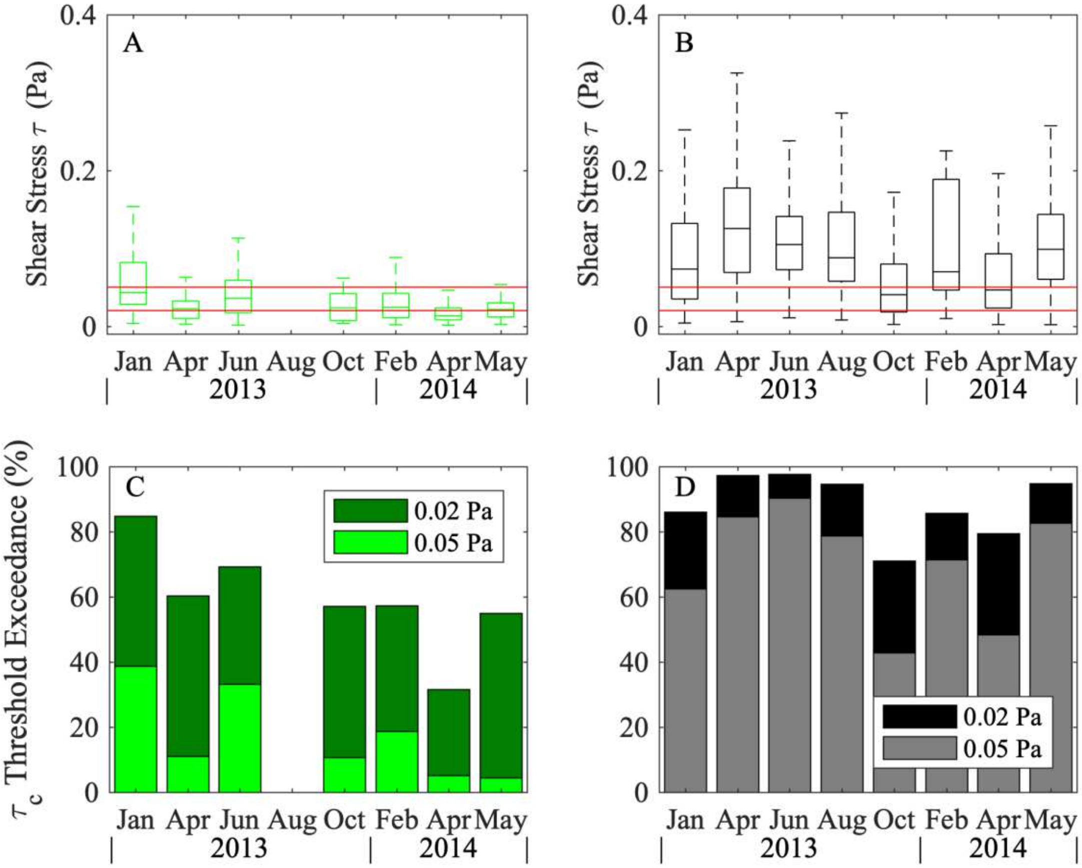
A
B
C
D
Shear Stress τ (Pa)
Shear Stress τ (Pa)
0.4
0.2
0
τ_c Threshold Exceedance (%)
100
80
60
40
20
0
0.02 Pa
0.05 Pa
Jan
Apr
Jun
Aug
Oct
Feb
Apr
May
2013
2014

Figure 7

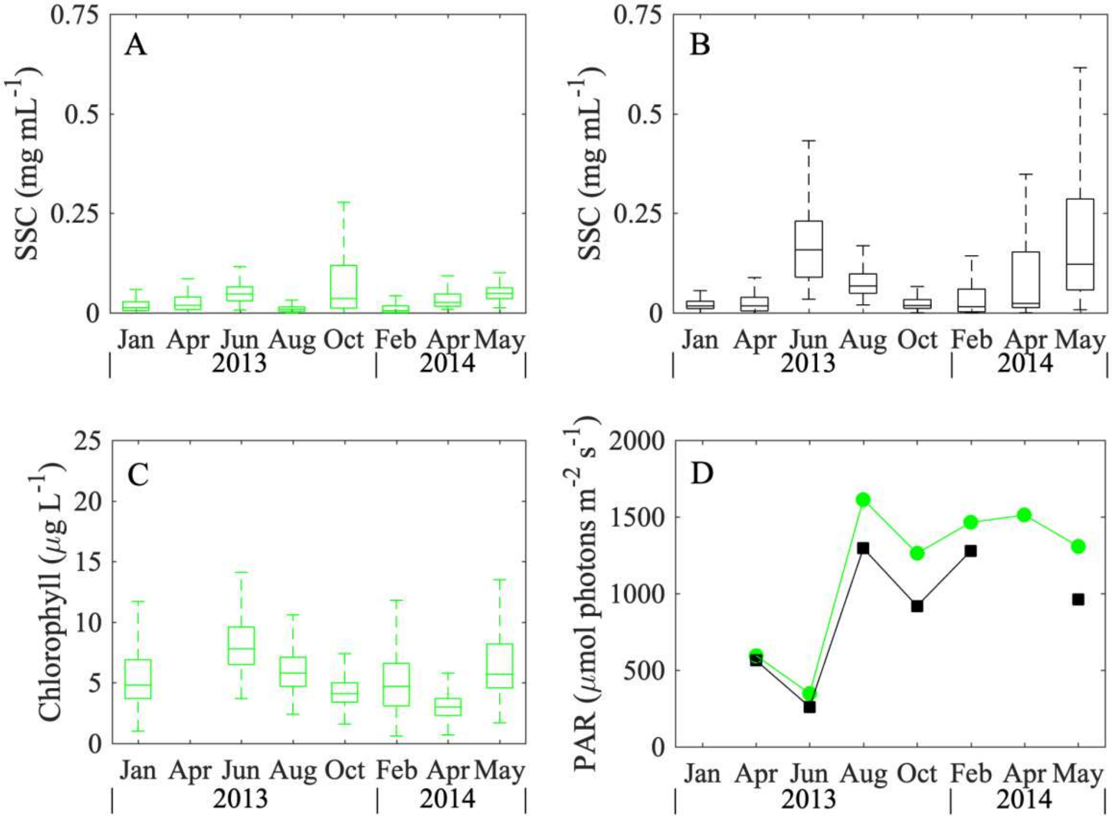
A
SSC (mg mL^{-1})
0.75
0.5
0.25
0
Jan Apr Jun Aug Oct Feb Apr May
2013
2014
B
SSC (mg mL^{-1})
0.75
0.5
0.25
0
Jan Apr Jun Aug Oct Feb Apr May
2013
2014
C
Chlorophyll (μg L^{-1})
25
20
15
10
5
0
Jan Apr Jun Aug Oct Feb Apr May
2013
2014
D
PAR (μmol photons m^{-2} s^{-1})
2000
1500
1000
500
0
Jan Apr Jun Aug Oct Feb Apr May
2013
2014

Figure 8

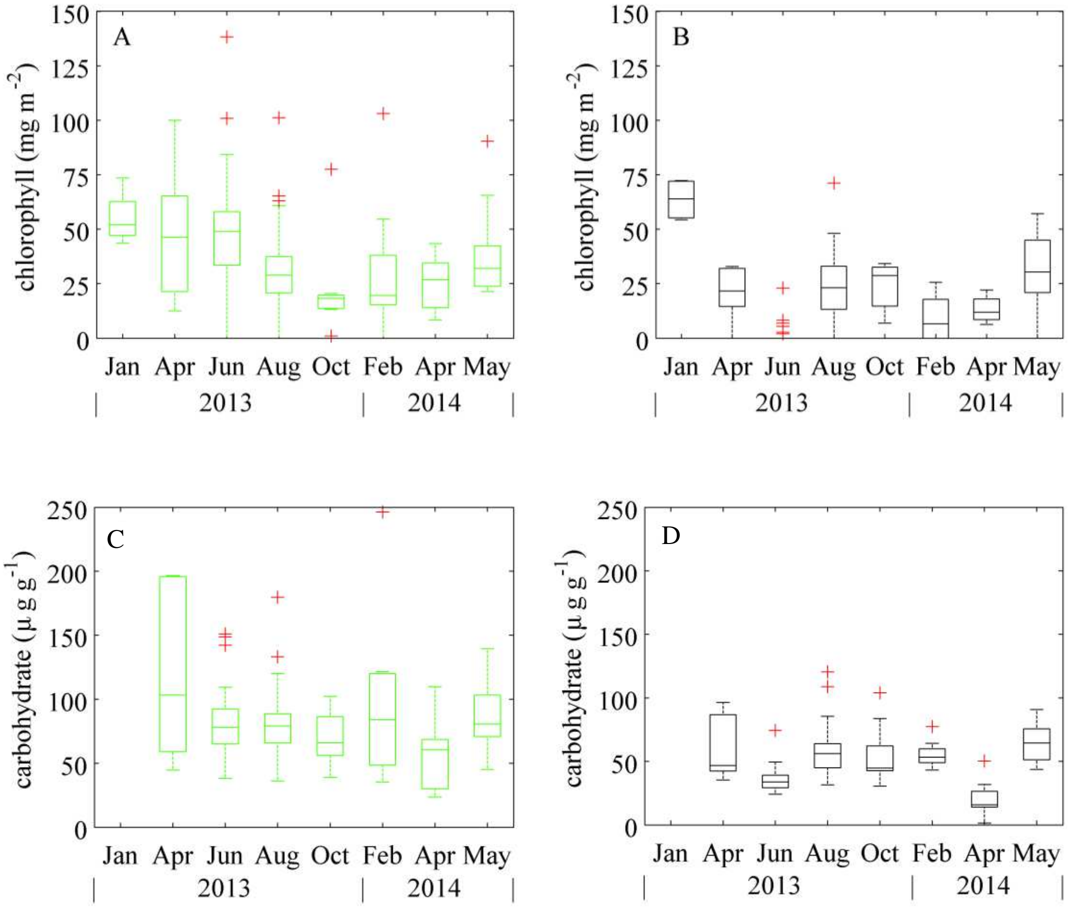
A
B
C
D
chlorophyll (mg m^{-2})
carbohydrate (µ g g^{-1})
0
25
50
75
100
125
150
200
250
Jan
Apr
Jun
Aug
Oct
Feb
Apr
May
2013
2014

Figure 9

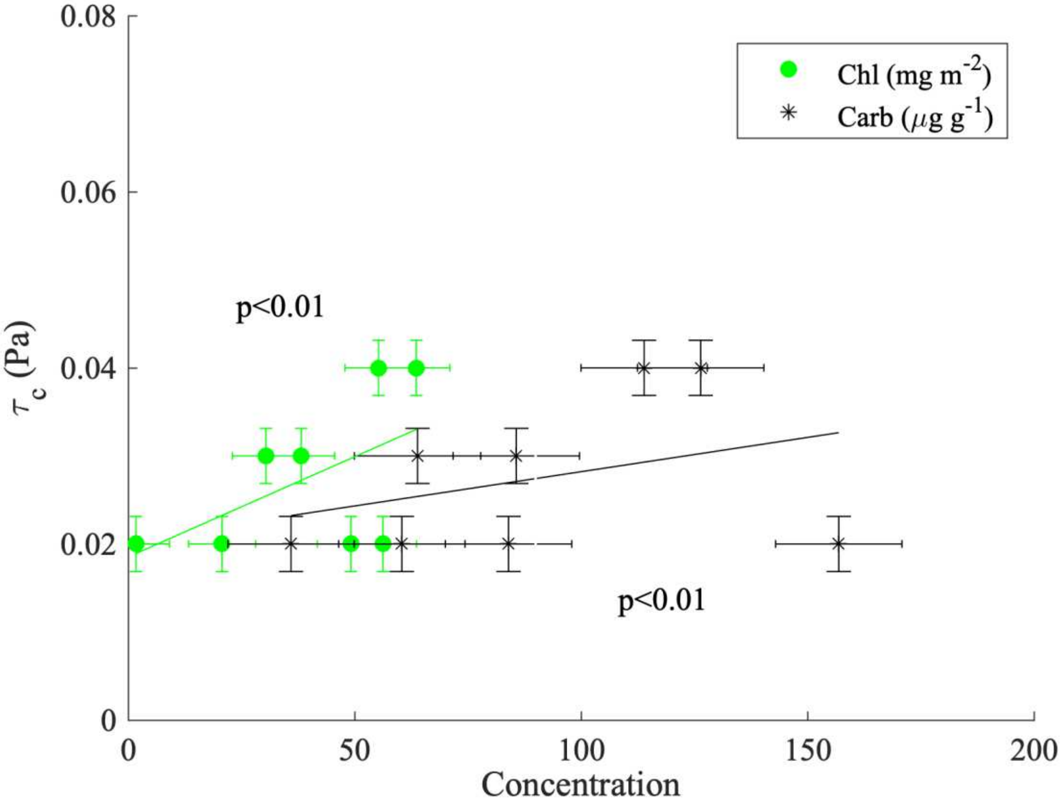

0.08
0.06
0.04
0.02
0
τ_c (Pa)
0
50
100
150
200
Concentration
● Chl (mg m^{-2})
* Carb (μg g^{-1})
p<0.01
p<0.01